European Journal of Medical Genetics 64 (2021) 104333

Contents lists available at ScienceDirect

European Journal of Medical Genetics

journal homepage: www.elsevier.com/locate/ejmg

Child to adulthood clinical description of MDPL syndrome due to a novel variant in *POLD1*

Battisti Gladys [a], Wintjens René [b], Decottignies Anabelle [c], Merhi Ahmad [d], Fervaille Caroline [e], Sokal Etienne [f], Karadurmus Deniz [a], Benoit Valerie [a], Claessens Anick [g], Martinet Jean-Paul [j], Martiat Benoît [h], Kinzinger Philippe [i], Maystadt Isabelle [a,k,*]

[a] *Centre for Human Genetics, Institut de Pathologie et de Génétique, Charleroi, Gosselies, Belgium*
[b] *Laboratory of Microbiology, Bioorganic and Macromolecular Chemistry, Université Libre de Bruxelles, Brussels, Belgium*
[c] *Telomeres Research Group, Genetic & Epigenetic Alterations of Genomes, de Duve Institute, Université catholique de Louvain, Brussels, Belgium*
[d] *IPG BioBank and Laboratory of Translational Oncology, Institut de Pathologie et de Génétique/Grand Hôpital de Charleroi, Gosselies, Belgium*
[e] *Department of Anatomopathology, Cliniques de Mont-Godinne, CHU-UCL-Namur, Godinne, Belgium*
[f] *UCLouvain, Cliniques Universitaires St Luc, Service de Gastroentérologie et Hépatologie Pédiatrique, 10 Av Hippocrate, Bruxelles, Belgium*
[g] *Department of Endocrinology, Vivalia, Cliniques Sud Luxembourg, Arlon, Belgium*
[h] *Department of Oto-Rhino-Laryngology, Vivalia, Cliniques Sud Luxembourg, Arlon, Belgium*
[i] *Department of Orthopedic Surgery, Vivalia, Cliniques Sud Luxembourg, Arlon, Belgium*
[j] *Department of Hepato-Gastro-Enterology, Cliniques de Mont-Godinne, CHU-UCL-Namur, Godinne, Belgium*
[k] *Faculty of Medicine, Unamur, Namur, Belgium*

ARTICLE INFO

Keywords:
MDPL syndrome
POLD1
Lipodystrophy
Progeroid features
CysB motif

ABSTRACT

Mandibular hypoplasia, Deafness, Progeroid features, and Lipodystrophy (MDPL) syndrome is a rare autosomal dominant disorder caused by mutations in *POLD1* gene and characterized by mandibular hypoplasia, deafness, progeroid features and lipodystrophy. One recurrent mutation p.(Ser605del) was reported in almost all affected patients.

We report a novel *de novo* c.3214A>C p.(Thr1072Pro) variant in *POLD1* in a 28-year-old male with MDPL syndrome. We provide a clinical description, molecular/immunohistological results, and literature review.

1. Introduction

The *POLD1* gene (OMIM #174761), located on chromosome 19q13.3-q13.4, encodes the delta DNA polymerase p125 catalytic subunit (Netz et al., 2012; Nicolas et al., 2016; Prindle and Loeb, 2012). With POLD2, POLD3 and POLD4, POLD1 forms the DNA polymerase delta (DNA Pol δ), an enzyme found in eukaryotes and involved in DNA replication and DNA damage repair.

POLD1 contains an exonuclease domain and a polymerase domain. It also has a CysA motif (Zn finger) and CysB motif (4Fe–4S cluster) in the C-terminal domain strongly conserved among DNA polymerase and species (Nicolas et al., 2016)Nicolas et al., 2016.

In 2010, Shastry et al. clinically described seven patients with mandibular hypoplasia, deafness, progeroid features, lipodystrophy and hypogonadism with undescended testes in males, which is described by the acronym MDPL syndrome (OMIM #615381) (Shastry et al., 2010a). In 2013, a recurrent heterozygous single-codon deletion in the polymerase domain of *POLD1* was identified in four patients with MDPL syndrome (Weedon et al., 2013). So far, 23 patients have been diagnosed with MDPL syndrome and an identified *POLD1* mutation, with 18 patients showing the recurrent p.Ser605del mutation, two patients harbouring the p.Arg507Cys missense mutation, two patients from the same family sharing the p.Glu1067Lys missense mutation and finally one patient with a severe phenotype showing the p.Ile1070Asn missense mutation.

We report on a patient with highly suggestive characteristics of MDPL syndrome in whom the sequencing of the *POLD1* gene revealed the novel *de novo* c.3214A>C p.(Thr1072Pro) variant in the C-terminal domain.

* Corresponding author. Centre de Génétique Humaine, Avenue Georges Lemaitre 25, B-6041, Gosselies, Belgium.
E-mail address: isabelle.maystadt@ipg.be (M. Isabelle).

https://doi.org/10.1016/j.ejmg.2021.104333
Received 2 March 2021; Received in revised form 12 August 2021; Accepted 2 September 2021
Available online 10 September 2021
1769-7212/

2. Material and methods

2.1. Patient selection and molecular method

The patient was referred for genetic counselling, as he was suspected to have an underlying syndromic aetiology. Written informed consent for publication was obtained in accordance with institutional guidelines.

Based on the patient's phenotype, a diagnosis of MDPL syndrome was clinically suspected. As the *POLD1* gene was included in our hereditary cancer panel, mutation analysis of *POLD1* gene was carried out by NGS on whole blood extracted DNA samples from the proband and his parents, with Illumina MiSeq technology, according to the manufacturer's protocol. Then, the variant was confirmed by PCR and direct Sanger sequencing using standard methods. The primer sequences and reaction conditions are available on request. The variant was interpreted and classified according to the ACMG 2015 guidelines (Richards et al., 2015).

2.2. Immunofluorescence

The derived lymphoblastoid cells of the patient were fixed in 4% PFA at RT for 10 min, washed with PBS and cells were adhered to poly-L-lysine coated glass slides by cytospin. Cells were subsequently permeabilized with 0.3% Triton X-100 in PBS for 5 min. Cells were blocked with 5% normal goat serum (Cell Signaling) in PBS for 1 h and then incubated with anti-NUP98 (Cell Signaling #2598T) or anti-lamin A/C (Cell Signaling #4777T) antibodies overnight at 4 °C. Slides were washed and incubated with anti-rabbit or anti-mouse (Alexa Fluor 488 or Alexa Fluor 594 Conjugate, Cell Signaling, 1:250) for 1 h at room temperature. After washing, the cells were mounted with an antifade mounting medium with DAPI (Vector Laboratories).

2.3. Western blot

Proteins were extracted from patients' derived lymphoblastoid cell cultures in RIPA buffer (Thermofisher) supplemented with phosphatases and protease inhibitors (cell signaling), and Western blotting was performed using standard protocol. Equal amounts of total cell protein (15 μg per lane) were electrophoresed on SDS–polyacrylamide gradient gels (4–15% mini-protean TGX gel, Bio-Rad Laboratories) and transferred to nitrocellulose membranes (Amersham). The primary antibodies used were: monoclonal POLD1 (ab186407; Abcam) and GAPDH (#sc-365062, Santa Cruz). The primary antibodies were detected with horseradish-peroxidase-conjugated anti-rabbit (#7074, cell signaling) or anti-mouse IgG (#7076, cell signaling) secondary antibodies followed by measurement of chemiluminescence (Lumi-Light PLUS, Roche Applied Science).

2.4. Structural analysis

In order to figure out the effects of mutation on the protein structure and function, the experimental structure of human DNA Pol δ enzyme was visualized and analysed through Coot 0.9 (Emsley et al., 2010). We used the structure of the DNA Pol δ tetramer solved at 3.08 Å resolution in ternary complex with double stranded DNA and proliferating cell nuclear antigen (PCNA) (PDB id 6TNY) (Lancey et al., 2020). Interface areas between subunits of the DNA Pol δ were analysed with the PISA sever tool (Krissinel and Henrick, 2007). Images of the 3D structure were generated using PyMol (The PyMol Molecular Graphics System, Version 2.3.0 Schrödinger, LLC).

3. Results

3.1. Clinical report

The proband was referred to our Clinical Genetics Centre in a context of a complex clinical association of progeroid facial appearance, lipodystrophy, truncal obesity, deafness, cryptorchidism with hypogonadism, joint stiffness, osteopenia, and mild cognitive impairment.

He is the second child of non-consanguineous healthy Caucasian parents. The brother is healthy (Supplementary Fig. 1).

The proband was born at term by vaginal delivery, after an uneventful pregnancy. He had a low birth weight (2840 g; - 0.9 DS) but normal height (50 cm; 0 DS) and head circumference (35 cm; 0 DS). The neonatal period was marked by poor feeding and low weight gain.

At 3 months, he presented with jaundice, which led to the diagnosis of alpha-1-antitrypsin deficiency (genotype ZZ), which was treated by ursodeoxycholic acid. To date, there is no complication, such as cirrhosis or emphysema. Psychomotor development was slightly delayed with acquisition of independent walking at 17 months and pronunciation of the first words at 2.5 years. The speech delay was attributed to bilateral sensorineural hearing loss in all frequencies but predominant at the medium frequencies. He wore hearing aids, which were not well tolerated until adolescence. He had learning and memory difficulties. A neuropsychological test performed at 10 years old showed a harmonious profile with a total IQ of 65, confirming mild intellectual disability. Since infancy, he is described as a shy and introverted boy, with a tendency to social isolation, but without typical autistic features. He had bilateral undescended testes with hypergonadotropic hypogonadism.

Since the age of 10, he progressively developed an emaciated face and slender limbs, with a gradual loss of subcutaneous tissue. Conversely, he developed truncal obesity, contrasting with the lipodystrophic appearance of the limbs and the face (Fig. 1). Since the age of 13 years, the proband wore glasses for myopia complicated by myopic choroidosis. He also has exophoria and exophthalmia. On the orthopaedic level, dorsal kyphosis and lumbar hyperlordosis were diagnosed. In childhood, he had hyperlaxity of the small joints. He progressively complained about joint stiffness, muscle cramps and chronic asthenia.

On clinical exam at 16 years of age, the proband had a weight of 53.5 kg (- 1 DS) with a height of 172 cm (- 0.5 DS), with a body mass index at 18 kg/m^2 (- 1 DS). His head circumference and arm spam/height ratio were in the normal range. He showed light hair, an emaciated face, exophthalmia, beaked nose, short philtrum, retrognathia with hypoplastic mandible, small ears (- 2 DS) (slightly dysplastic and in posterior rotation), slender limbs and translucent skin. The distribution of subcutaneous tissue was abnormal, with a deficit of adipose tissue in the limbs and an accumulation of fat around the abdomen. He had abdominal stretch marks. He had dorsal kyphosis and generalized joint stiffness. His shoulder elevation was limited. Mobilisation of elbows and knees were painful. He showed arachnodactyly in his feet and hands (length of middle fingers >2 DS). Cardiopulmonary auscultation was normal, as was examination of the abdomen. There was no hepatosplenomegaly. Patellar osteotendinous reflexes were brisk but symmetrical (Fig. 1). Blood tests revealed mild hepatic cytolysis (GOT 58 UI/L and GPT 133 UI/L, n.v. 45 and 57 respectively) without cholestasis, hypergonadotropic hypogonadism with LH 13.4 mUI/mL (n.v. 1.7–12.1), FSH 24.7 mUI/mL (n.v. 1.4–9.9), and testosterone 10 nM (n.v 10–35). Metabolic assessment, including analyses of plasma and urinary amino acid profiles, was normal. Osteopenia, requiring treatment with calcium and vitamin D, was documented by bone densitometry. Skin biopsy was normal on optic microscopy. Cardiac and carotid ultrasounds revealed no anomalies. The abdominal ultrasound showed a liver with irregular edges and hyperechoic appearance.

On the genetic level, CGH-array analysis (Agilent ISCA 44k) was performed and showed a 257 kb microduplication in the 3q26.2 region, which was inherited from his mother and likely benign. The sequencing analysis of *TGFβR1*, *TGFβR2, FBN1* and *SKI* genes revealed no pathogenic mutations.

From the age of 17, the proband began to experience scarring in the knees. Joint stiffness increased with tendon retractions. For his hypogonadism, he received a monthly injection of testosterone (Sustanon ®).

At the age of 26 years, the patient was re-evaluated by the geneticist.

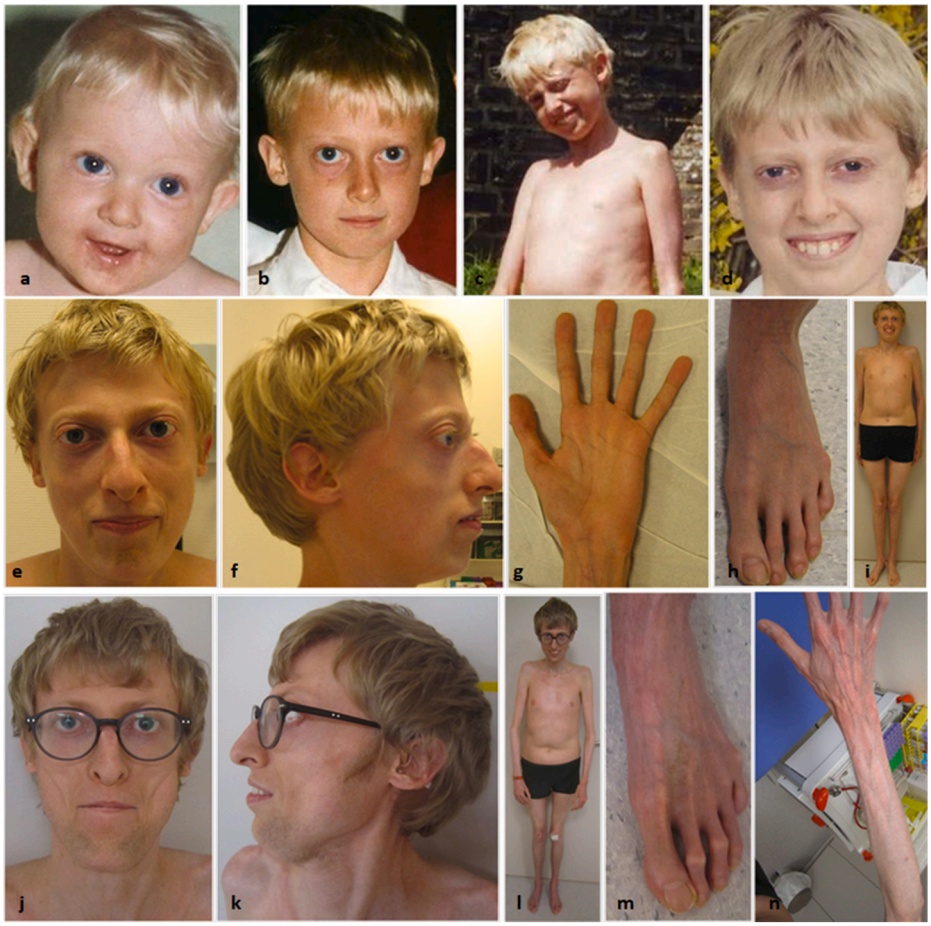

Fig. 1. Clinical characteristics of the patient. (a–d): Patient at the age of 1 year (a), 7.5 years (b), 10 years (c) and 11.5 years (d). We note the absence of specific dysmorphic features during infancy. Since the age of 10, the patient showed a progressive emaciated face, dental crowding and an overweight trunk with thin limbs suggestive of lipodystrophy. (e–i): Patient at 16 years of age with typical characteristics of MDPL syndrome, such as bird-like facies, beaked nose, prominent eyes, mandibular hypoplasia, muscle wasting and thin skin. (j–n): Patient at 27 years of age with additional signs of overall premature ageing, notably telangiectasias and joint contractures. The lipodystrophy and the other morphological and facial characteristics previously noted are more pronounced.

His weight was 50.2 kg (- 2.5 DS) with a height of 172.7 cm (−0.7 DS), giving a body mass index at 16.95 kg/m^2 (- 3 DS). His clinical features were accentuated compared to the previous consultation, with a very emaciated face, a near absence of subcutaneous fatty tissue in the limbs and a prominent abdomen. His facies had a progeroid aspect. His skin was extremely thin. He had a nasal and high-pitched voice. He had significant dental overcrowding (Fig. 1). The liver was palpated 1 cm below the right costal margin. The blood sample analysis revealed increased hepatic cytolysis with GOT at 75 UI/L and GPT at 179 UI/L, still without signs of cholestasis. The carbohydrate evaluation showed a fasting glucose, C-peptide and insulin within the standards. However, the lipid evaluation was abnormal with a non-HDL cholesterol increased to 111 mg/dL (standards <100). The increases in LH and FSH levels were less pronounced, and the testosterone level was normalized to 13 nM under Sustanon treatment. A liver biopsy showed chronic hepatitis with not only an appearance compatible with alpha-1-antitrypsin deficiency but also steatohepatitis of unknown aetiology in the context of an absence of toxic consumption (Supplementary Fig. 1).

3.2. Genetic findings

The sequencing analysis of the *POLD1* gene (NM_001256849.1) highlighted the presence at the heterozygous state of the c.3214A>C p.(Thr1072Pro) variant (Chr19(GRCh38): g.50920522 A>C). The ClinVar accession number is SCV001468507. This variant was not found in the parents, suggesting that it arose *de novo* (Supplementary Fig. 2).

This missense substitution concerns a nucleotide and an amino acid highly conserved among the species within the protein domain "C4-type zinc finger of DNA polymerase delta". To our knowledge, this variant has never been described in the literature nor has it been observed in control population databases (gnomAD).

According to the ACMG recommendations (Richards et al., 2015), the variant was considered as likely pathogenic due to the association of PS2 (*de novo* with both maternity and paternity confirmed in a patient with the disease and no familial history), PM1 (located in a well-established functional domain), PM2 (absent from control databases), PP2 (missense variant in a gene that has a low rate of benign missense variation and in which missense variants are a common mechanism of disease) and PP4 (patient's phenotype highly specific for a disease with a single genetic aetiology) criteria.

By Western blot, the study of the protein expression level of mutated POLD1 in the lymphoblastoid-derived cells of the patient showed no difference in comparison with controls of same age (Fig. 2).

To complete the genetic investigations, we studied the telomere length using flow-FISH (Baerlocher et al., 2006), which was slightly above the P50 for the patient in comparison with that in the general population (data not shown).

Analysis of the nuclear membrane on derivated lymphoblastoid cells by immunofluorescence labelling with anti-NUP98 and anti-lamin A/C did not show any difference between our patient and two controls of similar age (Fig. 3).

3.3. Structural interpretation

The complete tetrameric structure of the human DNA Pol δ has recently been elucidated by cryogenic electron microscopy (cryo-EM) (Lancey et al., 2020), allowing us to visualize the variant residue in the three-dimensional structure of the enzyme and subsequently the forecasting of its structural impacts upon mutation. The variant residue p125.Thr1072 is localized within the vicinity of the CysB motif, next to

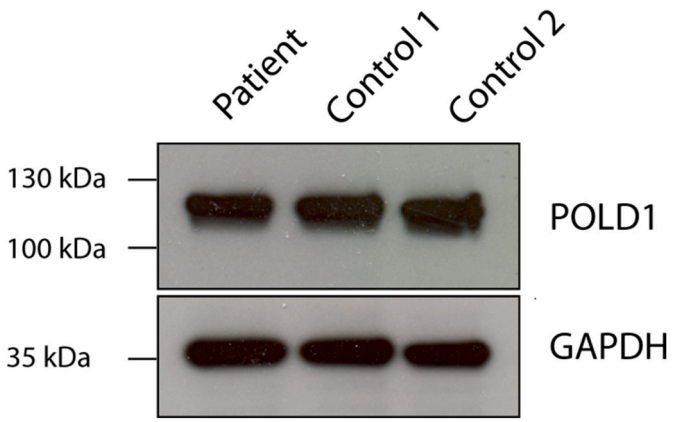

Fig. 2. Western Blot from lymphoblastoid cells protein extracts.
Western blot study of POLD1 expression in the patient vs two controls showed no significant difference.

Cys1071 (the third cysteine involved in the metal coordination of the 4Fe–4S cluster) (Fig. 4a). However, this residue does not take part directly in the 4Fe–4S binding site, as its side chain is directed towards the subunit p12 of DNA Pol δ (encoded by *POLD4*) (Fig. 4b). Therefore, Thr1072 is partially hidden by the subunit p12, with 37% of its solvent accessible surface buried in the p125-p12 subunit interface. In the cryo-EM structure, the side chain of Thr1072 is found in contact with p125.Phe1079 and with the last two residues of the p12 subunit, Pro106 and Ile107 (Fig. 4b). Of note, Thr1072 is also likely to interact with unmodeled residues 485–490 of p125, as evidenced by the cryo-EM maps (Supplementary Fig. 3).

Two scenarios can be envisaged when replacing the threonine in position by a proline, an amino acid adding conformational constraints and thereby reducing the local flexibility of the polypeptide chain. First, destabilization of the 4Fe–4S cluster due to the immediate proximity of the chelating Cys1071, and second, an effect on the binding of p12 as Thr1072 is part, albeit to a lesser extent, of the interface between the two subunits p125 and p12.

4. Discussion

MDPL syndrome belongs to the very heterogeneous group of lipodystrophy disorders and is caused by heterozygous mutations within the *POLD1* gene, suggesting a mechanism of haploinsufficiency or a negative dominant effect (Sasaki et al., 2018). This syndrome is classically characterized by a normal weight, size and appearance at birth. The progressive loss of subcutaneous fat and abnormal distribution of adipose tissue occur gradually in late childhood, around the first decade. Lipodystrophy is frequently associated with various progressive metabolic disorders, such as insulin resistance, diabetes mellitus, dyslipidaemia and fatty liver disease (Ajluni et al., 2017; Reinier et al., 2015). The dysmorphic signs found in MDPL syndrome are mandibular hypoplasia, prominent eyes, a beaked nose, a narrow mouth with dental overcrowding, a progeroid appearance and thin skin (sometimes with telangiectasias). The voice is high-pitched. Patients also frequently exhibit joint contractures, premature osteoporosis, thoracic kyphosis and scoliosis. Hearing impairment occurring during the first or second decade of life is one of the key symptoms of MDPL, but some exceptions have been described (Chen et al., 2017; Elouej et al., 2017; Okada et al., 2017; Pelosini et al., 2014; Reinier et al., 2015; Shastry et al., 2010a; Sasaki et al., 2018; L. R. Wang et al., 2018; Weedon et al., 2013). The median age of diagnosis is around 20 years of age, with the various clinical characteristics of the syndromes adding up over time and making the diagnosis clinically possible (Okada et al., 2017). Fertility does not seem to be affected in women, as shown by two cases of vertical

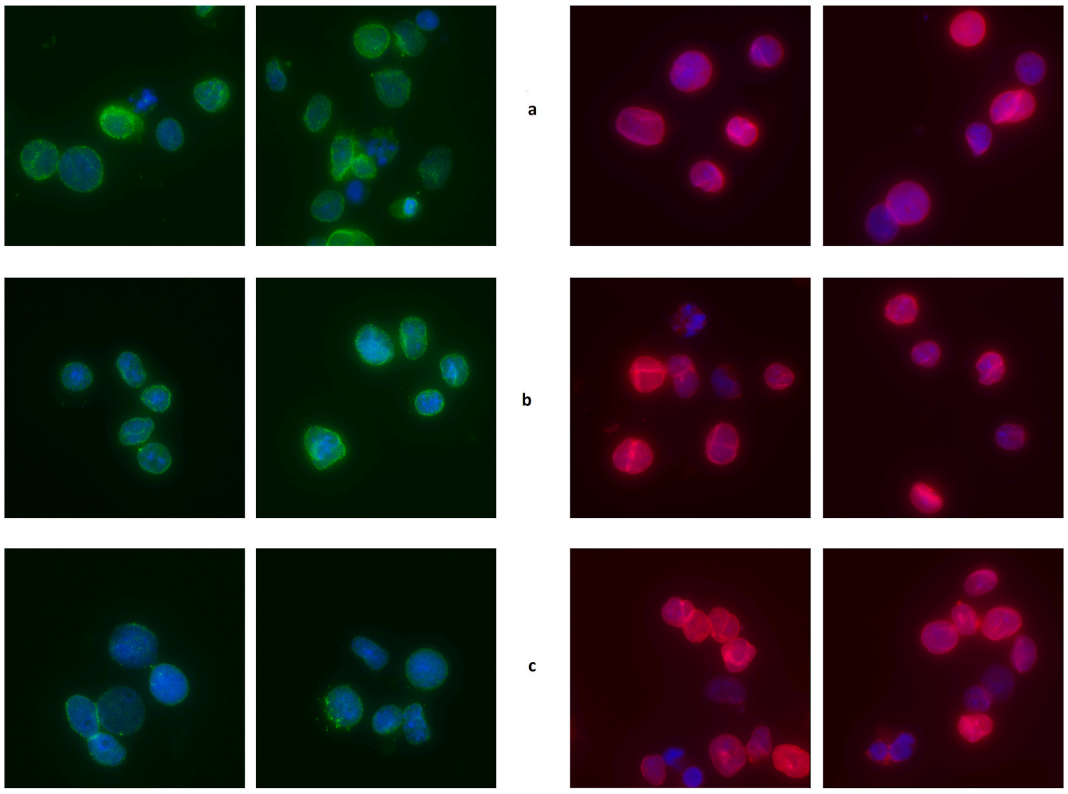

Fig. 3. Nuclear membrane immuno-staining.
Nuclear labelling of lymphoblastoid cells by immunofluorescence with anti-NUP98 (right) and anti-lamin A/C (left) antibodies in the patient (a) showed no abnormal nuclear shape and no difference in comparison with two controls (b and c) of the same sex and age.

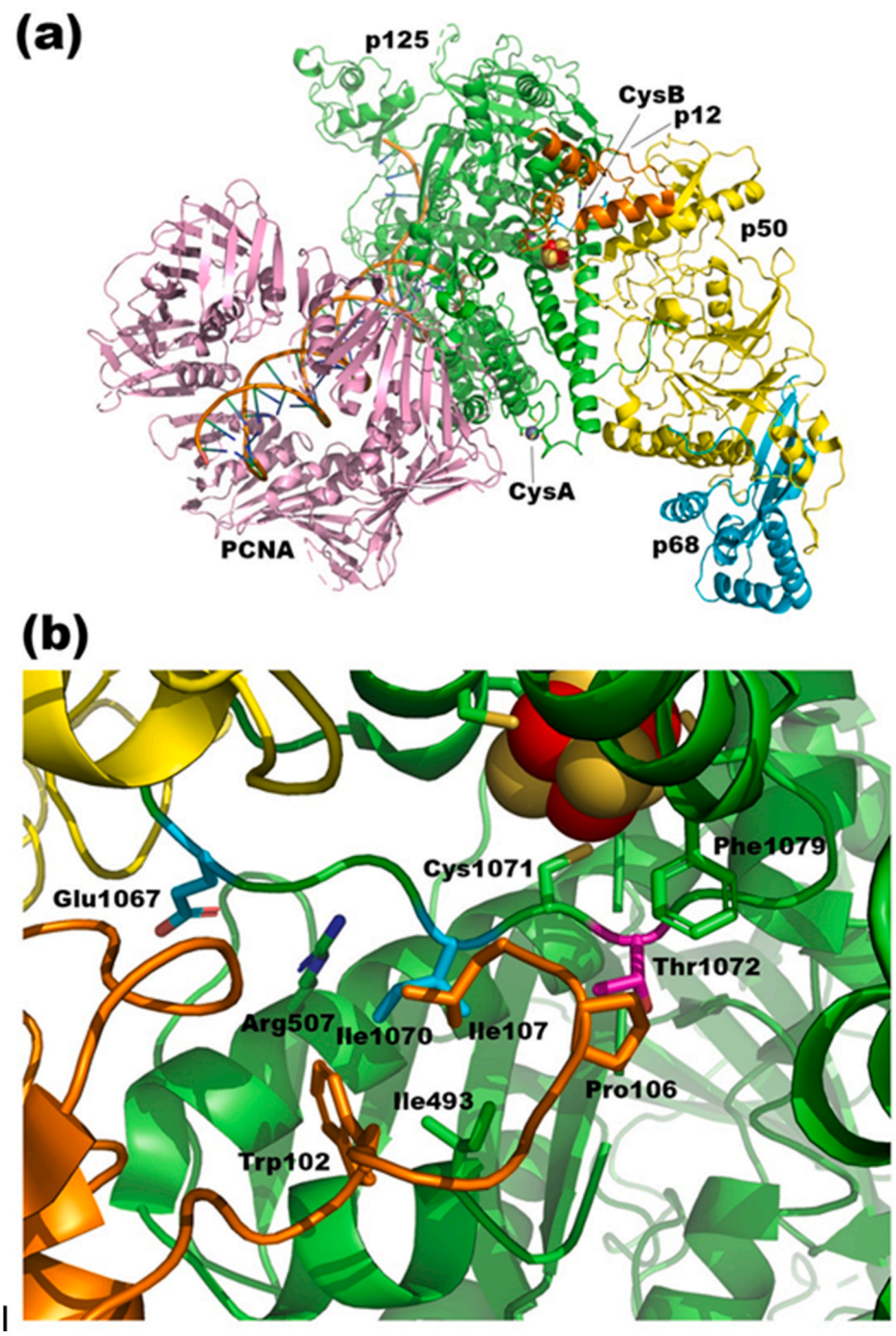

Fig. 4. Mapping the POLD1 mutation residues on the 3D structure of DNA Pol δ. **(a)** General view of the cryo-EM structure of DNA Pol δ tetramer bound to DNA and PCNA (PDB id 6TNY). Proteins are depicted as ribbons coloured in green, yellow, cyan, orange and pink for POLD1 (p125/Polδ1), POLD2 (p50/Polδ2), POLD3 (p68/Polδ3), POLD4 (p12/Polδ4) and PCNA, respectively. DNA is shown with the ribose-phosphate backbone as orange coils and nucleotide rings as sticks. The CysA and CysB motifs are labelled. The Zn ion of CysA motif is depicted as a grey sphere, while the 4Fe–4S cluster of CysB is depicted as spheres coloured in red and yellow for iron and sulphur, respectively. The mutation residues, Glu1067, Ile1070 and Thr1072, are in stick representation with carbon atoms in magenta for the latter and in cyan for the two former ones. Cysteine residues of the CysA and CysB motifs, as well as residues interacting with the three mutation residues are also in stick representation with carbon atoms coloured according the corresponding protein ribbon colour. In stick representation, nitrogen, oxygen and sulphur atoms are in blue, red and yellow, respectively.
(b) Close-up view of the region around the residue Thr1072. All residues in stick representation are labelled. . (For interpretation of the references to colour in this figure legend, the reader is referred to the Web version of this article.)

transmission of the *POLD1* mutation (Lessel et al., 2015). However, all women with MDPL syndrome have poor breast development. Some have micropolycystic ovaries, and one patient developed secondary amenorrhoea after 3 years of regular cycles. Affected men show cryptorchidism with hypergonadotropic hypogonadism (Sasaki et al., 2018; Shastry et al., 2010a). It is more difficult to give a prognosis to their fertility, given the absence of offspring in the identified male patients. Many patients with MDPL syndrome have been described with short stature, as in other progeroid syndromes (Lessel et al., 2015). A Chinese patient with the Ser605del *POLD1* mutation was described with short stature, hypogonadism and IGF1 deficiency (Chen et al., 2017). After GH therapy in this context and in the absence of a molecular diagnosis, he showed an acceleration of the loss of subcutaneous fat. Indeed, GH stimulates the lipolysis of adipose tissue and consequently causes the release of free fatty acid into the blood, which leads to dysfunction and apoptosis of the β cells of the pancreas. By its mechanisms, it accelerates the loss of subcutaneous adipose tissue and worsens the metabolic manifestations found in MDPL syndrome, such as insulin resistance, diabetes mellitus and hypertriglyceridaemia. Therefore, treatment with GH is not recommended in MDPL syndrome (Chen et al., 2017). Finally, there does not seem to be an increased predisposition to cancers or shortened life expectancy (Sasaki et al., 2018; Wang et al., 2020), although a very severe MDPL syndrome phenotype with premature death in the context of recurrent respiratory infections was described in a patient with a p.Ile1070Asn mutation (Elouej et al., 2017).

Our patient presents with lipodystrophy, progeroid aspect, hearing loss, cryptorchidism, joint contractures, kyphosis, thin skin and psychological fragility described in MDPL syndrome. To date, he has no

metabolic disorder, such as hyperinsulinism, glucose intolerance or dyslipidaemia. However, his steatohepatitis can be attributed to MDPL syndrome rather than to his alpha-1-antitrypsin deficiency. Table 1 summarizes the various symptoms/clinical features highlighted in patients with MDPL syndrome reported in the literature according to their genotype and compared to our patient.

Some phenotypic features of MDPL syndrome are shared with other progeroid syndromes, such as Hutchinson-Gilford (OMIM #176670) syndrome due to *LMNA* mutations, Werner syndrome (OMIM # 277700) linked to *WRN* mutations and mandibuloacral dysplasia (MAD) (OMIM #248370) syndrome secondary to *LMNA* or *ZMPSTE24* mutations. However, severe failure to thrive and short life expectancy (found in Hutchinson-Gilford syndrome) (Hennekam, 2006), premature hair loss and juvenile cataracts (typical of Werner syndrome) (Wang et al., 2018), or clavicular dysplasia and acroosteolysis (classically described in MAD) are not found in MDPL syndrome (Lessel et al., 2015; Reinier et al., 2015). Additional progeroid syndromes have been described. Nestor-Guillermo progeria syndrome, due to *BANF1* biallelic mutations and described in 3 patients to date, is characterized by the absence of metabolic and cardiovascular abnormalities but a particularly severe and disabling skeletal phenotype (Fisher et al., 2020; Puente et al., 2011). A severe form of Mandibuloacral syndrome (also called MADaM) has been described in 7 patients with biallelic mutations of *MTX2*. (Elouej et al., 2020). Table 2 compares the clinical characteristics of MDPL syndrome with these progeroid syndromes.

The *POLD1* gene is located on chromosome 19q13.3-q13.4. Its main transcript includes 27 exons and produces an 1107 amino acid protein. This protein constitutes the p125 catalytic subunit of one of the main replicative DNA polymerases: Pol δ. Pol δ is a tetramer whose catalytic unit p125 has a 3′-5′ exonuclease activity domain (amino acids 304 to 533) and a 5′-3′ polymerase activity domain (amino acids 579 to 974). It also has a CysA motif (Zn finger; amino acids 1012–1029) and CysB motif (4Fe–4S cluster; amino acids 1058–1076) in the C-terminal domain (Nicolas et al., 2016). The CysB motifs are strongly conserved among all replicative DNA polymerases and among all species. It is essential to allow the stability of the binding with the DNA strand and to allow an adequate interaction of the catalytic subunit with the corresponding accessory subunit, which are both necessary for the polymerase activity of the enzyme (Netz et al., 2012). Therefore, thanks to its polymerase and exonuclease activities, POLD1 plays an essential role in the regulation of cell cycle, DNA synthesis and DNA damage repair processes (Song et al., 2015; J. L. Wang et al., 2012). POLD1 is expressed ubiquitously in all tissues and decreasingly during life, making it a potential actor in cell senescence and ageing (Nicolas et al., 2016; Prindle and Loeb, 2012; Wang et al., 2018). It has been demonstrated that E2F1 and CCCTC-binding factor (CTCF) act as transcription factors for POLD1 expression regulation. With age, the levels of CTCF and E2F1 expression decrease and the binding affinity of E2F1 for the POLD1 promoter declines in reverse proportion with the increasing methylation of CpG island 3, therefore contributing to cellular aging (Gao et al., 2019; Hou et al., 2021). Like *POLD1,* the other genes related to progeroid syndromes also play critical roles in cell division and the protection of genetic information (Shastry et al., 2010a). More particularly, the *WRN* gene encodes for a helicase interacting with POLD1 during DNA replication and repair processes, which may explain the common manifestations of these syndromes (Lessel et al., 2015; Sasaki et al., 2018). However, to date, the physiopathological link with the metabolism of adipose tissue remains poorly understood (Lessel et al., 2015; Sasaki et al., 2018). In Hutchinson-Gilford syndrome, which is characterized by the abnormal accumulation of progerin resulting from aberrant splicing and processing of lamin A, accelerated telomere shortening has been well described and seems to be an important part of the explanation to cell ageing and progeria phenotype (Aguado et al., 2019; Allsopp et al., 1992; Benson et al., 2010; Decker et al., 2009; Kudlow et al., 2008). However, the measurement of telomere lengths in our patient did not show any abnormalities and suggests other physiopathological mechanisms for the cell ageing and progeria features in MDPL syndrome. The *BANF1* gene plays a role in nuclear assembly and the organization of chromatin (Fisher et al., 2020; Puente et al., 2011; Segura-Totten et al., 2002). Finally, *MTX2*-mutated patient fibroblasts displayed mitochondrial network fragmentation and respiratory chain dysfunction, confirming that mitochondrial dysfunction is also involved in cellular senescence (Elouej et al., 2020).

Heterozygous germline mutations within the exonuclease domain of the *POLD1* gene have been implicated in a predisposition to colorectal polyposis and endometrial cancer (Palles et al., 2013; Nicolas et al., 2016; Prindle and Loeb, 2012; Wang et al., 2018). Otherwise, a recurrent mutation (p.Ser605del) within the polymerase activity domain of POLD1 has been implicated the MDPL syndrome. This mutation occurs in a very conserved area of the polymerase activity domain, which is involved in the incorporation of dNTPs for the extension of DNA primers and in the formation of phosphodiester bonds. *In vitro* functional expression studies in *E. coli* confirmed its pathogenic character by showing an abolition of the polymerase activity and a partial decrease of the exonuclease activity in the mutant Ser605-deletion. Furthermore, it was demonstrated that the Ser605del mutant was able to bind DNA but unable to catalyse polymerization, being responsible for the stalled replication forks, double-stranded DNA breaks and genomic instability involved in ageing and cell death (Wang et al., 2018; Weedon et al., 2013). Lately, Fiorillo et al. confirmed the presence of nuclear envelope abnormalities, the presence of micronuclei and the accumulation of pre-lamin A in fibroblasts of patients with MDPL compared to control cells. They also found a reduced capacity to repair DNA damage in MDPL fibroblasts, as found in other progeroid syndromes (Fiorillo et al., 2018). This offers the possibilities of pathophysiological explanations for MDPL syndrome (Fiorillo et al., 2018; Weedon et al., 2013). With the immunohistochemistry analysis of our patient's lymphoblastoid cells culture, we could not detect any nuclear membrane shape abnormalities (Fig. 3). These structural changes may be tissue/cell-specific. Unfortunately, we could not obtain fibroblasts from our patient to confirm this hypothesis. The simplified explanation that mutations in the exonuclease domain are responsible for an oncogenic phenotype, and mutations in the polymerase domain result in MDPL syndrome has been invalidated by the identification of the missense mutation p.Arg507Cys within the exonuclease domain in two patients with MDPL syndrome (Lessel et al., 2015; Pelosini et al., 2014). Furthermore, more recently, two missense mutations within the C-terminal domain (CysB motif), p.Glu1067Lys and p.Ile1070Asn, have been described in three patients with MDPL syndrome but a variable phenotypic expression (Ajluni et al., 2017; Elouej et al., 2017). The first mutation, p.Glu1067Lys, was identified in a mother and daughter with a slight phenotype associating lipodystrophy, a small jaw without mandibular hypoplasia and the absence of progeroid features. However, they showed severe metabolic disorders, such as insulin resistance and dyslipidaemia (Ajluni et al., 2017). The second mutation, p.Ile1070Asn, was described in a young woman with an extremely severe phenotype, who died at 25 years from respiratory failure in a context of bulbar dysphagia and major scoliosis. She had lipodystrophy, facial dysmorphism and major growth retardation compared to the previous patients. Due to the absence of a molecular diagnosis before the patient's death, her metabolic status could not be more fully investigated. Elouej et al. predicted *in silico* that the substitution p.Ile1070Asn has an impact on the secondary structure of the protein and on the accessibility of the amino acid chains of this region, more particularly on the residues Cys1071 and Cys1076, which allow the formation of the 4Fe–4S cluster. In this way, it is likely that this variant induces a loss of the polymerase activity of DNA Pol δ and consequently MDPL syndrome (Elouej et al., 2017).

Our patient harbours the novel *de novo* heterozygous c.3214A>C p.(Thr1072Pro) variant in *POLD1*. By Western Blot analysis performed from our patient's lymphoblastoid derived cell cultures, we showed that the level of expression of the mutated POLD1 is similar to controls (Fig. 2). The c.3214A>C p.(Thr1072Pro) variant is located in the

Table 1
Clinical characteristics of previously reported patients with MDPL syndrome-related POLD1 mutations and comparison with our patient.

	Weedon et al.	Weedon et al.	Weedon et al.	Weedon et al.	Pelosini et al.	Reinier et al.	Lessel et al.	Lessel et al.	Leel et al.	Lessel et al.	Lessel et al.	Lessel et al.	Lessel et al.	Lessel et al.
Age (age first feature)	23	37	19	25	48 (5)	41(3)	30 (12)	28	17 (12)	18	39	10	10 (4)	62
Sex	Male	Male	Female	Male	Female	Female	Female	Female	Female	Male	Female	Male	Female	Male
Ethnicity	British	British	Italian	Indian	Caucasian	Italian	US and European	French	Columbian	Swedish	French	French	Hungarian	US and European
Mutation	p. Ser605del	p. ser605del	p. Ser605del	p. Ser605del	R507C	p.Ser605del	p.Ser605del	Ser605del	Ser605del	Ser605del	Ser605del	Ser605del	Ser605del	R507C
Birth weight (Z score)	4.2 kg (1.6)	3.6 kg (0.5)	3.8 kg (1.2)	3 kg (−0.7)	3.6 kg (0.8)	NA	2.41 kg (−1.9)	2.65 kg (−1.4)	NA	NA	NA	2.56 kg (−1.7)	3.3 kg (0.1)	NA
Weight (Z score)	69.7 kg (−0.1)	51 kg (−2.4)	45 kg (−1.9)	41.2 kg (−4.3)	47.8 kg (−1.4)	33 kg (−5.4)	54.4 kg (0.43)	34 kg (−5.0)	31 kg (−2.3)	39.1 kg (−4.5)	37 kg (−3.9)	21 kg (−3.1)	31 kg (−0.3)	66 kg (−0.4)
Height (Z score)	1 m 91 (2)	1 m 76 (−0.1)	1 m 60 (−0.5)	1 m 68 (−1.2)	1 m 62 (−0.2)	1 m 45 (−2.8)	1 m 57 (−1)	1 m 57 (−1)	1 m 30 (−3.7)	1 m 62 (−1.95)	1 m 48 (−2.4)	1 m 23 (−2.4)	1 m 45 (1)	1 m 57 (−2.8)
BMI kg/m^2 (Z score)	19.1 (−1.7)	16.5 (−3.4)	17.6 (−1.8)	14.6 (−5.3)	18.2 (−1.4)	15.7 (−3.2)	21.9 (0.1)	13.8 (−5.3)	18.3 (−1.4)	14.9 (−4.3)	16.9 (−2.2)	13.9 (−1.9)	14.7 (−1.2)	26.8 (1)
Lipodystrophy	Y	Y	Y	Y	Y	Y	Y	Y	Y	NA	Y	Y	Y	Y
Muscle wasting	NA	NA	NA	NA	NA	Y	Y	Y	N	Y	Y	N	Y	Y
Tight and thin skin	Y	Y	Y	Y	Y	Y	Y	Y	Y	Y	Y	Y	Y	Y
Bird-like facies	Y	Y	Y	Y	Y	Y	NA	NA	NA	NA	NA	NA	NA	NA
Beaked nose	NA	NA	NA	NA	Y	Y	NA	NA	Y	Y	Y	NA	Y	Y
Prominent eyes	NA	NA	NA	NA	Y	Y	NA	NA	NA	NA	NA	NA	Y	NA
Progeroid facial features	NA	NA	NA	NA	Y	Y	NA	NA	NA	Y	Y	NA	Y	Y
Mandibular hypoplasia	Y	Y	Y	Y	Y	NA	Y	Y	Y	Y	Y	Y	Y	N
Dental overcrowding	Y	Y	Y	Y	Y	N, prominent	N	Y	Y	N	Y	Y	Y	N
High-pitched voice	Y	Y	Y	Y	NA		N	N	Hoarse	N	Hoarse	Y	Y	Y
Premature greying or loss of hair	NA	NA	NA	NA	NA	N	Y (loss)	N	N (thin)	N	Y (greying)	N	N	Y (greying)
Joint contracture	Y	Y	Y	Y	NA	Y	NA	NA	NA	NA	NA	NA	Y	NA
Kyphosis/ scoliosis	Y	Y	N	Y	Y	NA	NA	NA	NA	NA	NA	NA	NA	NA
Osteopenia	Y	Y	N	Y	NA	NA	N	Y	Y	N	N	N	N	NA
Hypogonadism (age at menarche)	Y	Y	N	Y	N (14)	Y (14,during 3–4 yrs)	N (11)	N (13)	N (12)	N	N (15)	Cryptorchidism	N	N
Undescended testes	Y	Y	NA	Y	NA (normal gonads)	NA	NA	NA	NA	NA	NA	NA	NA	NA
Breast development	NA	NA	NA	NA	Poor	Poor	NA	NA	NA	NA	NA	NA	NA	NA
Deafness (age at diagnosis)	Y (12)	Y (33)	Y (7)	Y (16)	Y (25)	Y (10)	N	Y (12)	Y (11)	N	Y (14)	Y (14)	N	Y
Cognitive function	Normal	Normal	Normal	Normal	Normal	Normal	Normal	Normal	Normal	NA	Normal	Normal	Normal	
Family history	N	N	N	N	N	N	Son	N	Mother	N	Son (confirmed)	Mother (confirmed)	N	N
	Y (14)	Y (37)	N	Y (23)	Y	Y (29)	Y (28)	N	N	N	N	N	N	Y (43)

(*continued on next page*)

Table 1 (*continued*)

	Weedon et al.	Weedon et al.	Weedon et al.	Weedon et al.	Pelosini et al.	Reinier et al.	Lessel et al.	Lessel et al.	Leel et al.	Lessel et al.	Lessel et al.	Lessel et al.	Lessel et al.	Lessel et al.
Diabetes (age at diagnosis)														
Fasting glucose (mg/dL)	90	121	76	139	95	NA	84	76	93	NA	94	84	76	93
OGTT 2 h glucose (mg/dL)	290	267	160	295	184	NA	NA	NA	NA	NA	NA	NA	NA	NA
Fasting insulin (pmol/L)	212	NA	235	169	236	NA	High	NA	NA	NA	NA	NA	Normal	NA
Hepatic steatosis	Y (16yrs)	NA	Y (16yrs)	N	Y	Y	Y	NA	NA	NA	NA	NA	N	NA
Hepatomegaly	N	N	Y	N	Y	Y	Y	NA	NA	NA	NA	NA	NA	NA
Total cholesterol (mg/dL)	206	210	214	164	NA	214	175	171	227	NA	226	NA	116	174
Triglycerides	131	142	230	149	High	331	215	190	NA	NA	218	Normal	212	232
Other						Microdactyly Depression, anxiety	Hypothyroidism		Ovarian cancer died age 34					Osteomyelitis, adrenal adenoma, cardiac Depression, anxiety

	Ajluni et al.	Ajluni et al.	Elouej et al.	Elouej et al.	Okada et al.	Chen et al.	Sasaki et al.	Wang et al.	Fiorillo et al.	The proband	Number of patients (average)/ Frequency
Age (age first feature)	34	14	24 (7)	6 (5)	11(3)	10 (4)	45 (5.5)	36 (1.5)	8 (2)	**27 (6)**	**(First feature: 5.7 years)**
Sex	Female	Female	Female	Male	Male	Male	Female	Male	Female	**Male**	**(11 M/13)**
Ethnicity	White-Hispanic	White-Hispanic	British	British	Japanese	Chinese	Japanese	Sicilian	Pakistani	**Belgian**	
Mutation	p.E1067K	p.E1067K	p.Ile1070Asn	p. Ser605del	p. Ser605del	p. Ser605del	p.Ser605del	p.Ser605del	p. Ser605del	**p. Thr1072Pro**	
Birth weight (Z score)	NA	NA	2.7 kg (−1.2)	3.18 kg (−0.4)	2.69 kg (−0.8)	3.2 kg (−0.3)	3.65 kg (−0.9)	NA	NA	**2 kg 830 (-0.9)**	
Weight (Z score)	53 kg (−0.6)	50.4 kg (−0.1)	12.6 kg (−36.2)	16.2 kg (−2)	24.6 kg (−2.4)	21.5 kg (−2.9)	30.8 kg (−6.4)	39.5 kg (−4.8)	NA	**50.2 kg (-2.5)**	
Height (Z score)	1 m 71 (1.2)	1 m 63 (−0.4)	1 m 20 (−6.6)	1 m 11 (−0.9)	1 m 25 (−2.4)	1 m 25 (−2.1)	1 m 42 (−3.3)	1 m 62 (−2.1)	NA	**1 m 72 (-0.7)**	
BMI kg/m^2 (Z score)	18.3 (−1.5)	19 (−0.1)	8.8 (−20)	13.09 (−2.5)	15.7 (−0.8)	13.8 (−2)	15.1 (−3.6)	15.1 (−4.7)	NA	**16.95 (-3)**	**(16.4)**
Lipodystrophy	Y	Y	Y	Y	Y	Y	Y	Y	Y	**Y**	**23/23 (100%)**
Muscle wasting	Y	NA	Y	NA	Y	Y	Y	Y	Y	**Y**	**15/17 (88%)**
Tight skin	Y	Y	Y	NA	Y	Y	Y	Y	Y	**Y**	**23/23 (100%)**
Bird-like facies	NA	NA	Y	Y	NA	Y	Y	NA	NA	**Y**	**10/10 (100%)**
Beaked nose	NA	NA	Y	Y	Y	Y	Y	NA	Y	**Y**	**14/14 (100%)**
Prominent eyes	NA	NA	Y	NA	Y	Y	Y	Y	NA	**Y**	**9/9 (100%)**
Progeroid facial features	Y	Y	Y	Y	NA	NA	Y	Y	NA	**Y**	**13/13 (100%)**
Mandibular hypoplasia	NA	NA	Y	Y	Y	Y	Y	Y	Y	**Y**	**19/20 (95%)**
Dental overcrowding	NA	NA	Y	Y	Y	Y	Y	Y	NA	**Y**	**17/21 (81%)**
High-pitched voice	NA	NA	Y	Y	Y	Y	Y	Y	NA	**Y**	**14/19 (74%)**

(*continued on next page*)

Table 1 (*continued*)

	Ajluni et al.	Ajluni et al.	Elouej et al.	Elouej et al.	Okada et al.	Chen et al.	Sasaki et al.	Wang et al.	Fiorillo et al.	The proband	Number of patients (average)/ Frequency
Premature greying or loss of hair	NA	NA	N	Y	NA	N	Y (alopecia)	N	NA	**N**	**5/15 (33%)**
Joint contracture	Y	NA	Y	Y	Y	Y	Y	Y	Y	**Y**	**15/15 (100%)**
Kyphosis/scoliosis	NA	NA	Y	N	N	N	NA	NA	NA	**N**	**5/10 (50%)**
Osteopenia	NA	NA	Y	N	NA	Y	Y	Y (9)	NA	**Y**	**10/17 (59%)**
Hypogonadism (age at menarche)	N (PCOS)	NA	Y	?	Y	Y	Y (13 yrs, oligo/ amenorrhoea)	Y	N	**Y**	**10/20 (50%)**
Undescended testes	NA	NA	NA	Unilateral	Y	Y	NA	NA	NA	**Y**	**7/7 (100%)**
Breast development	Poor	Poor	Poor	NA	NA	NA	NA	NA	NA	**NA**	**5/5 (100%)**
Deafness (age at diagnosis)	N	N	N	Y(4)	Y (7)	Y (8)	Y (8–9)	Y (10)	Y (2)	**Y (2.5)**	**18/24 (75%) Mean age = 11.5 yrs**
Cognitive function	Bipolar disorder	Dyslexia	Normal	Normal	Normal	Normal	Depressive state	Normal	Normal	**Borderline IQ shy**	**6/23 (26%)**
Family history	Daughter	Mother	N	N	N	N	N	Wernet (four brothers)	NA	**N**	**6/24 (25%)**
Diabetes (age at diagnosis)	Y	Y	NA	N	N	N	Y (IGT 21 yrs, DM 33 yrs)	N	IGT	**N**	**11/23 (48%) Mean age = 29.6 yrs**
Fasting glucose (mg/dL)	NA	NA	151	<101	NA	69.55	High	NA	NA	**NA**	
OGTT 2 h glucose (mg/dL)	NA	NA	NA	NA	NA	84.5	NA	NA	NA	**NA**	
Fasting insulin (pmol/L)	NA	NA	NA	357	NA	42.1	High	NA	High	**NA**	
Hepatic steatosis	Y	Y	N	N	Y	N	Y (21)	Y	NA	**Y**	**11/16 (69%) Mean age = 17.7 yrs**
Hepatomegaly	NA	NA	N	N	NA	NA	NA	NA	NA	**Y**	**5/10 (50%)**
Total cholesterol (mg/dL)	NA	NA	NA	113	141	166.2	227	284	NA	**NA**	
Triglycerides	5194	7004	NA	Normal	125	Normal	153	785	NA	**NA**	
Other	Incontinence, recurrent pancreatitis, elevated CK	Rectal prolapse, brain abscess (secondary to otitis), pancreatitis	Death at age 25 (respiratory failure)				HTA and atherosclerosis		Anaemia	**NA**	

DM: diabetes mellitus; IGT: impaired glucose tolerance; NA: not available; N: no; Y: yes.

Table 2
Comparison of the clinical characteristics of MDPL syndrome with the other progeroid syndromes.

Clinicals Characteristics	Hutchinson-Gilford Progeria Syndrome	Werner Syndrome	Mandibuloacral dysplasia type A/B	MADaM syndrome	Nestor-Guillermo Progeria Syndrome	MDPL syndrome
Gene	*LMNA*	*RECQL2*	*LMNA/ZMPSTE24*	*MTX2*	*BANF1*	*POLD1*
Inheritance	AD/AR	AR	AR	AR	AR	AD
Onset	Early infancy	Early adulthood	Childhood	Infancy/early childhood	Infancy/early childhood	Early childhood
Growth	Severe growth failure; short stature	Short stature	Postnatal growth retardation/short stature	Short stature, poor weight gain and microcephaly	Short stature/failure to thrive	Normal
Facial dysmorphology	• Prematurely aged face • Large head for face • Beaked nose • Retrognathia and micrognathia • Thin lips • Delayed dental eruption and dental crowding • Alopecia	• Prematurely aged face • Beaked nose • Pinched facial features • Premature greying and/or thinning hair	• Prematurely aged face • Beaked nose • Mandibular hypoplasia • Bird-like face • Prominent eyes • Hypoplastic teeth/dental overcrowding • Alopecia	• Mandibular hypoplasia • Beaked nose • Small mouth • Alopecia • Amelogenesis imperfecta • Dental overcrowding	• Prematurely aged faced • Beaked nose • Micrognathia/midface hypoplasia • Mandibular osteolysis • Dental overcrowding • Scalp hair sparse to absent since 2nd decade of life	• Prematurely aged face • Beaked nose • Mandibular hypoplasia • Bird-like facies • Prominent eyes • Small mouth • Dental overcrowding
Eyes, ears and voice	• Nocturnal lagophthalmos • Conductive hearing loss • High-pitched voice	• Cataracts and retinal degeneration • Voice change	• /	• Exophtalmia • One patient with corneal opacity	• Proptosis • Spares eyebrow and eyelashes	• Sensorineural deafness • High-pitched voice
Skin, skeletal and fat	• Scleroderma-like skin • Osteoporosis and multiple fractures • Generalized lipodystrophy	• Scleroderma-like skin/ chronic ulcers/subcutaneous calcification • Osteoporosis • Thin limbs	• Skin atrophy/subcutaneous calcification • Joint stiffness/contractures • Acroosteolysis of the clavicle and distal phalanges/clavicular hypoplasia • Generalized (B) or partial (A) lipodystrophy	• Skin atrophy • Hyper/hypopigmentation • Osteoporosis/osteopenia • Acroostelysis of distal phalanges, clavicular hypoplasia, hip dysplasia • Delayed closure of cranial suture • Lipodystrophy	• Skin atrophy • Patchy hyperpigmentation • Generalized lipoatrophy • Joint stifness/contracture • Osteoporosis • Osteolysis of clavicules/ribs • Scoliosis	• Tight skin/scleroderma-like skin/telangiectasias • Osteoporosis/joint contracture • Generalized lipodystrophy with increased visceral fat
Metabolic issues	• No puberty and no cases of fertility • Insulin resistance without diabetes mellitus	• Type 2 diabetes mellitus • Hypogonadism • Early decline of fertility	• Type 2 diabetes mellitus and impaired glucose tolerance	• Metabolic syndrome	• None	• Type 2 diabetes mellitus • Hypogonadism
Cardiac/vascular features	• Cardiac dysfunction • Severe atherosclerosis • AIT/AVC	•Severe atherosclerosis	Variable	• Mitral valve prolapsus • Left ventricular hypertrophy • High blood pressure and renal glomerulosclerosis	• No atherosclerosis • Sinus tachycardia/Right bundle branch block • Pulmonary hypertension (secondary to scoliosis)	Variable
Neoplasia	Not increased	Increased	Not increased	• Not described	• Not described	Not increased
Laboratory Abnormalities	• Serum leptin concentrations low • Shortened telomere	• A lot of translocation mosaicism in cultured fibroblasts	• Hyperglycaemia • Hyperlipidaemia • Hyperinsulinaemia	• Proteinuria	• Low leptin level • Low 25-OH-vitamin D level • Low fasting glucose (in some patients)	• Abnormal liver function tests • Hypertryglyceridaemia
Life expectancy	• 13.4 years	• 54 years	• Seems normal	• Second decade	• 30 years	• Seems normal
Other	• Dystrophic nails	/	• Delayed closure of cranial sutures • Dystrophic nails	• Hepatomegaly/steatosis • Recurrent pulmonary infection • Developmental delay/hypotonia – normal cognitive function	/	• Poor breast development • Cryptorchidism

vicinity of two previously described mutations, p.Glu1067Lys and p.Ile1070Asn. Ile1070 and Thr1072 surround the Cys1071 of the CysB motif, both residues having their side chain pointing towards the subunit p12 and interacting with the C-terminal part of this subunit (Fig. 4a). The side chain of Ile1070 is found in contact with Trp102 (nearest distance of 3.6 Å) and Ile107 (3.8 Å) of p12 (Fig. 4b). Therefore, it is likely that the two variants p.Thr1072Pro and p.Ile1070Asn give similar phenotypes, through partial destabilization of the 4Fe–4S cluster and/or subtle changes in the binding interface of the p12 subunit. Accordingly, it has been proposed that point mutations in the CysB motif alter DNA polymerase and/or exonuclease activities and confer an error-prone phenotype due to structural alterations in the 4Fe–4S cluster environment (Jozwiakowski et al., 2019). Of note, whereas the p.Thr1072Pro variant confers local conformational constraints to the peptide chain, the p.Ile1070Asn variant places a polar amino acid in a hydrophobic environment. In contrast, Glu1067 was more distant from the CysB motif (i.e., distance ~14 Å), and the variant p.Glu1067Lys is expected to cause a different structural change. In the structure of the DNA Pol δ heterotetramer, the side chain of p125.Glu1067 points towards the p50 subunit and makes a salt bridge with p125.Arg507 (Fig. 4b). As the Glu1067Lys mutation changes the net negative charge to a positive one, an electrostatic repulsion will take place resulting in local destabilization of the structure, thereby impairing the protein function. The p12 subunit is involved in modulation of the rate and fidelity of DNA synthesis. In the presence of p12, DNA synthesis is faster, whereas in its absence, the proofreading activity of the enzyme is increased (Meng et al., 2010). Indeed, in response to DNA damage by UV and alkylating chemicals, as well as under replication stress, p12 is transiently degraded, resulting in the DNA Pol δ heterotetramer, a high-fidelity and low lesion-bypass enzyme (Lee et al., 2017). As Thr1072 contributes to the protein-protein interface with p12, its change by a proline amino acid might alter the p125/p12 binding and possibly might compromise the regulation of DNA Pol δ by degradation of p12. However, based only on the cryo-EM structure, it remains difficult to deduce how the p125/p12 binding is altered (i.e., increased or decreased), and therefore, how the regulation of DNA Pol δ might be disturbed by the mutation p.Thr1072Pro. An *in vitro* characterization of the protein variants could shed light on these questions.

In conclusion, we describe a patient with typical features of MDPL syndrome caused by a novel *de novo* heterozygous c.3214A>C p.(Thr1072Pro) variant in the CysB motif within the C-terminal domain of *POLD1*. MDPL syndrome shows a variable phenotype and its natural history still remains poorly known. The description of a larger number of patients would help to establish more readable genotype/phenotype correlations, as well as to specify life expectancy, the natural history of the disease, the recommended monitoring and the therapeutic possibilities. With the implementation of the whole genome sequencing technique in clinical genetics labs, the age of the molecular diagnosis of MDPL syndrome could drastically decrease. As the phenotype is not easily recognizable in young patients, the report of novel pathogenic variants is important for the interpretation of NGS data in the future. The better characterization of the function of the POLD1 protein will improve the understanding of the pathophysiological mechanisms of lipodystrophy, cell ageing and the link between these two processes.

Declaration of competing interest

All authors state that they have no conflicts of interest.

Acknowledgements

We thank the patient and his family for their participation and consent. RW is a Research Associate with the Belgian National Funds for Scientific Research (FRS-FNRS).

Appendix A. Supplementary data

Supplementary data to this article can be found online at https://doi.org/10.1016/j.ejmg.2021.104333.

References

Aguado, J., Sola-Carvajal, A., Cancila, V., Revêchon, G., Ong, P.F., Jones-Weinert, C.W., Wallén Arzt, E., Lattanzi, G., Dreesen, O., Tripodo, C., Rossiello, F., Eriksson, M., d'Adda di Fagagna, F., 2019. Inhibition of DNA damage response at telomeres improves the detrimental phenotypes of Hutchinson–Gilford Progeria Syndrome. Nat. Commun. 10 (1), 4990. https://doi.org/10.1038/s41467-019-13018-3.

Ajluni, N., Meral, R., Neidert, A.H., Brady, G.F., Buras, E., McKenna, B., DiPaola, F., Chenevert, T.L., Horowitz, J.F., Buggs-Saxton, C., Rupani, A.R., Thomas, P.E., Tayeh, M.K., Innis, J.W., Omary, M.B., Conjeevaram, H., Oral, E.A., 2017. Spectrum of disease associated with partial lipodystrophy: lessons from a trial cohort. Clin. Endocrinol. 86 (5), 698–707. https://doi.org/10.1111/cen.13311.

Allsopp, R.C., Vaziri, H., Patterson, C., Goldstein, S., Younglai, E.V., Futcher, A.B., Greider, C.W., Harley, C.B., 1992. Telomere length predicts replicative capacity of human fibroblasts. Proc. Natl. Acad. Sci. U.S.A. 89 (21), 10114–10118. https://doi.org/10.1073/pnas.89.21.10114.

Baerlocher, G.M., Vulto, I., de Jong, G., Lansdorp, P.M., 2006. Flow cytometry and FISH to measure the average length of telomeres (flow FISH). Nat. Protoc. 1 (5), 2365–2376. https://doi.org/10.1038/nprot.2006.263.

Benson, E.K., Lee, S.W., Aaronson, S.A., 2010. Role of progerin-induced telomere dysfunction in HGPS premature cellular senescence. J. Cell Sci. 123 (15), 2605–2612. https://doi.org/10.1242/jcs.067306.

Chen, T., Li, M., Wu, H., Xie, R., Wang, F., Chen, X., Sun, H., Chen, L., 2017. Short stature as the first manifestation of mandibular hypoplasia, deafness, progeroid features and lipodystrophy (MDPL) syndrome. Int. J. Clin. Exp. Med. 10 (2), 3876–3883.

Decker, M.L., Chavez, E., Vulto, I., Lansdorp, P.M., 2009. Telomere length in Hutchinson-Gilford progeria syndrome. Mech. Ageing Dev. 130 (6), 377–383. https://doi.org/10.1016/j.mad.2009.03.001.

Elouej, S., Beleza-Meireles, A., Caswell, R., Colclough, K., Ellard, S., Desvignes, J.P., Béroud, C., Lévy, N., Mohammed, S., Des Sandre-Giovannoli, A., 2017. Exome sequencing reveals a de novo POLD1 mutation causing phenotypic variability in mandibular hypoplasia, deafness, progeroid features, and lipodystrophy syndrome (MDPL). Metabolism: Clinical and Experimental 71, 213–225. https://doi.org/10.1016/j.metabol.2017.03.011.

Elouej, S., Harhouri, K., Le Mao, M., Baujat, G., Nampoothiri, S., Kayserili, H.U., Menabawy, N. Al, Selim, L., Paneque, A.L., Kubisch, C., Lessel, D., Rubinsztajn, R., Charar, C., Bartoli, C., Airault, C., Deleuze, J.F., Rötig, A., Bauer, P., Pereira, C., De Sandre-Giovannoli, A., 2020. Loss of MTX2 causes mandibuloacral dysplasia and links mitochondrial dysfunction to altered nuclear morphology. Nat. Commun. 11 (1), 4589. https://doi.org/10.1038/s41467-020-18146-9.

Emsley, P., Lohkamp, B., Scott, W.G., Cowtan, K., 2010. Features and development of Coot. Acta Crystallogr. Sect. D Biol. Crystallogr. 66 (4), 486–501. https://doi.org/10.1107/S0907444910007493.

Fiorillo, C., D'Apice, M.R., Trucco, F., Murdocca, M., Spitalieri, P., Assereto, S., Baratto, S., Morcaldi, G., Minetti, C., Sangiuolo, F., Novelli, G., 2018. Characterization of MDPL Fibroblasts Carrying the Recurrent p.Ser605del Mutation in POLD1 Gene. DNA Cell Biol. https://doi.org/10.1089/dna.2018.4335.

Fisher, H.G., Patni, N., Scheuerle, A.E., 2020. An additional case of Néstor-Guillermo progeria syndrome diagnosed in early childhood. Am. J. Med. Genet. A 182 (10), 2399–2402. https://doi.org/10.1002/ajmg.a.61777.

Gao, S., Song, Q., Liu, J., Zhang, X., Ji, X., Wang, P., 2019. E2F1 mediates the downregulation of POLD1 in replicative senescence. Cell. Mol. Life Sci. 76 (14), 2833–2850. https://doi.org/10.1007/s00018-019-03070-z.

Hennekam, R.C.M., 2006. Hutchinson-Gilford progeria syndrome: review of the phenotype. Am. J. Med. Genet.A 140 (23), 2603–2624. https://doi.org/10.1002/ajmg.a.31346.

Hou, Y., Song, Q., Gao, S., Zhang, X., Wang, Y., Liu, J., Fu, J., Cao, M., Wang, P., 2021. CTCF mediates replicative senescence through POLD1. Frontiers in Cell and Developmental Biology 9, 618586. https://doi.org/10.3389/fcell.2021.618586.

Jozwiakowski, S.K., Kummer, S., Gari, K., 2019. Human DNA polymerase delta requires an iron–sulfur cluster for high-fidelity DNA synthesis. Life Sci. Alliance 2 (4), e201900321. https://doi.org/10.26508/lsa.201900321.

Krissinel, E., Henrick, K., 2007. Inference of macromolecular assemblies from crystalline state. J. Mol. Biol. 372 (3), 774–797. https://doi.org/10.1016/j.jmb.2007.05.022.

Kudlow, B.A., Stanfel, M.N., Burtner, C.R., Johnston, E.D., Kennedy, B.K., 2008. Suppression of proliferative defects associated with processing-defective lamin A mutants by hTERT or inactivation of p53. Mol. Biol. Cell 19 (12), 5238–5248. https://doi.org/10.1091/mbc.E08-05-0492.

Lancey, C., Tehseen, M., Raducanu, V.S., Rashid, F., Merino, N., Ragan, T.J., Savva, C.G., Zaher, M.S., Shirbini, A., Blanco, F.J., Hamdan, S.M., De Biasio, A., 2020. Structure of the processive human Pol δ holoenzyme. Nat. Commun. 11 (1), 1109. https://doi.org/10.1038/s41467-020-14898-6.

Lee, M.Y.W.T., Wang, X., Zhang, S., Zhang, Z., Lee, E.Y.C., 2017. Regulation and Modulation of Human DNA Polymerase δ Activity and Function. Genes (Basel) 8 (7), 190. https://doi.org/10.3390/genes8070190.

Lessel, D., Hisama, F.M., Szakszon, K., Saha, B., Sanjuanelo, A.B., Salbert, B.A., Steele, P.D., Baldwin, J., Brown, W.T., Piussan, C., Plauchu, H., Szilvássy, J., Horkay, E., Högel, J., Martin, G.M., Herr, A.J., Oshima, J., Kubisch, C., 2015. POLD1 germline

mutations in patients initially diagnosed with werner syndrome. Hum. Mutat. 36 (11), 1070–1079. https://doi.org/10.1002/humu.22833.
Meng, X., Zhou, Y., Lee, E.Y.C., Lee, M.Y.W.T., Frick, D.N., 2010. The p12 subunit of human polymerase Δ modulates the rate and fidelity of DNA synthesis. Biochemistry 49 (17), 3545–3554. https://doi.org/10.1021/bi100042b.
Netz, D.J.A., Stith, C.M., Stümpfig, M., Köpf, G., Vogel, D., Genau, H.M., Stodola, J.L., Lill, R., Burgers, P.M.J., Pierik, A.J., 2012. Eukaryotic DNA polymerases require an iron-sulfur cluster for the formation of active complexes. Nat. Chem. Biol. 8 (1), 125–132. https://doi.org/10.1038/nchembio.721.
Nicolas, E., Golemis, E.A., Arora, S., 2016. POLD1: Central mediator of DNA replication and repair, and implication in cancer and other pathologies. Gene 590 (1), 128–141.
Okada, A., Kohmoto, T., Naruto, T., Yokota, I., Kotani, Y., Shimada, A., Miyamoto, Y., Takahashi, R., Goji, A., Masuda, K., Kagami, S., Imoto, I., 2017. The first Japanese patient with mandibular hypoplasia, deafness, progeroid features and lipodystrophy diagnosed via POLD1 mutation detection. Human Genome Variation 4, 17031. https://doi.org/10.1038/hgv.2017.31.
Palles, C., Cazier, J.B., Howarth, K.M., Domingo, E., Jones, A.M., Broderick, P., Kemp, Z., Spain, S.L., Almeida, E.G., Salguero, I., Sherborne, A., Chubb, D., Carvajal-Carmona, L.G., Ma, Y., Kaur, K., Dobbins, S., Barclay, E., Gorman, M., Martin, L., Rimmer, A., 2013. Germline mutations affecting the proofreading domains of POLE and POLD1 predispose to colorectal adenomas and carcinomas. Nat. Genet. 45 (2), 136–144. https://doi.org/10.1038/ng.2503.
Pelosini, C., Martinelli, S., Ceccarini, G., Magno, S., Barone, I., Basolo, A., Fierabracci, P., Vitti, P., Maffei, M., Santini, F., 2014. Identification of a novel mutation in the polymerase delta 1 (POLD1) gene in a lipodystrophic patient affected by mandibular hypoplasia, deafness, progeroid features (MDPL) syndrome. Metabolism: Clinical and Experimental 63 (11), 1385–1389. https://doi.org/10.1016/j.metabol.2014.07.010.
Prindle, M.J., Loeb, L.A., 2012. DNA polymerase delta in dna replication and genome maintenance. In: Environmental and Molecular Mutagenesis, , 9th53. 666, 682.
Puente, X.S., Quesada, V., Osorio, F.G., Cabanillas, R., Cadiñanos, J., Fraile, J.M., Ordóñez, G.R., Puente, D.A., Gutiérrez-Fernández, A., Fanjul-Fernández, M., Lévy, N., Freije, J.M.P., López-Otín, C., 2011. Exome sequencing and functional analysis identifies BANF1 mutation as the cause of a hereditary progeroid syndrome. Am. J. Hum. Genet. 88 (5), 650–656. https://doi.org/10.1016/j.ajhg.2011.04.010.
Reinier, F., Zoledziewska, M., Hanna, D, Smith, J.D., Valentini, M., Zara, I., Berutti, R., Sanna, S., Oppo, M., Cusano, R., Satta, R., Montesu, M.A., Jones, C., Cerimele, D., Nickerson, D.A., Angius, A., Cucca, F., Cottoni, F., Crisponi, L., I., 2015. Mandibular hypoplasia, deafness, progeroid features and lipodystrophy (MDPL) syndrome in the context of inherited lipodystrophies. Metabolism 64 (11), 1530–1540.
Richards, S., Aziz, N., Bale, S., Bick, D., Das, S., Gastier-Foster, J., Grody, W.W., Hegde, M., Lyon, E., Spector, E., Voelkerding, K., Rehm, H.L., 2015. Standards and guidelines for the interpretation of sequence variants: a joint consensus recommendation of the American college of medical genetics and genomics and the association for molecular pathology. Genet. Med. 17 (5), 405–424. https://doi.org/10.1038/gim.2015.30.
Sasaki, H., Yanagi, K., Ugi, S., Kobayashi, K., Ohkubo, K., Tajiri, Y., Maegawa, H., Kashiwagi, A., Kaname, T., 2018. Definitive diagnosis of mandibular hypoplasia, deafness, progeroid features and lipodystrophy (MDPL) syndrome caused by a recurrent de novo mutation in the POLD1 gene. Endocr. J. 65 (2), 227–238. https://doi.org/10.1507/endocrj.EJ17-0287.
Segura-Totten, M., Kowalski, A.K., Craigie, R., Wilson, K.L., 2002. Barrier-to-autointegration factor: major roles in chromatin decondensation and nuclear assembly. JCB (J. Cell Biol.) 158 (3), 475–485. https://doi.org/10.1083/jcb.200202019.
Shastry, S., Simha, V., Godbole, K., Sbraccia, P., Melancon, S., Yajnik, C.S., Novelli, G., Kroiss, M., Garg, A., 2010a. A novel syndrome of mandibular hypoplasia, deafness, and progeroid features associated with lipodystrophy, undescended testes, and male hypogonadism. Journal of Clinical Endocrinology and Metabolism 95 (10), E192–E197. https://doi.org/10.1210/jc.2010-0419.
Song, J., Hong, P., Liu, C., Zhang, Y., Wang, J., Wang, P., 2015. Human POLD1 modulates cell cycle progression and DNA damage repair. BMC Biochem. 16, 14. https://doi.org/10.1186/s12858-015-0044-7.
Wang, J.L., Guo, H.L., Wang, P.C., Liu, C.G., 2012. Age-dependent down-regulation of DNA polymerase δ1 in human lymphocytes. Mol. Cell. Biochem. 371 (1–2), 157–163. https://doi.org/10.1007/s11010-012-1432-6.
Wang, L.R., Radonjic, A., Dilliott, A.A., McIntyre, A.D., Hegele, R.A., 2018. A de novo POLD1 mutation associated with mandibular hypoplasia, deafness, progeroid features, and lipodystrophy syndrome in a family with werner syndrome. Journal of Investigative Medicine High Impact Case Reports 6. https://doi.org/10.1177/2324709618786770, 2324709618786770.
Wang, X.W., Lu, L.Y., Xie, Y., Yu, X.J., 2020. A Chinese girl with mandibular hypoplasia, deafness, progeroid features, and lipodystrophy (MDPL) diagnosed via POLD1 mutation detection. Chinese Med J 133 (16), 2009–2011. https://doi.org/10.1097/CM9.0000000000000986.
Weedon, M.N., Ellard, S., Prindle, M.J., Caswell, R., Allen, H.L., Oram, R., Godbole, K., Yajnik, C.S., Sbraccia, P., Novelli, G., Turnpenny, P., McCann, E., Goh, K.J., Wang, Y., Fulford, J., McCulloch, L.J., Savage, D.B., Rahilly, S.O., Kos, K., Hattersley, A.T., 2013. An in-frame deletion at the polymerase active site of POLD1 causes a multisystem disorder with lipodystrophy. Nat. Genet. 45 (8), 947–950. https://doi.org/10.1038/ng.2670.